INFECTION AND IMMUNITY, June 2005, p. 3577–3586 Vol. 73, No. 6
0019-9567/05/$08.00+0 doi:10.1128/IAI.73.6.3577–3586.2005
Copyright © 2005, American Society for Microbiology. All Rights Reserved.

Gamma Interferon-Induced T-Cell Loss in Virulent *Mycobacterium avium* Infection

Manuela Flórido,[1] John E. Pearl,[3] Alejandra Solache,[3] Margarida Borges,[1] Laura Haynes,[3] Andrea M. Cooper,[3] and Rui Appelberg[1,2]*

Laboratory of Microbiology and Immunology of Infection, Institute for Molecular and Cell Biology,[1] and Instituto de Ciências Biomédicas de Abel Salazar, University of Porto,[2] Porto, Portugal, and Trudeau Institute, Saranac Lake, New York[3]

Received 9 September 2004/Returned for modification 2 December 2004/Accepted 11 January 2005

Infection by virulent *Mycobacterium avium* caused progressive severe lymphopenia in C57BL/6 mice due to increased apoptosis rates. T-cell depletion did not occur in gamma interferon (IFN-γ)-deficient mice which showed increased T-cell numbers and proliferation; in contrast, deficiency in nitric oxide synthase 2 did not prevent T-cell loss. Although T-cell loss was IFN-γ dependent, expression of the IFN-γ receptor on T cells was not required for depletion. Similarly, while T-cell loss was optimal if the T cells expressed IFN-γ, $CD8^+$ T-cell depletion could occur in the absence of T-cell-derived IFN-γ. Depletion did not require that the T cells be specific for mycobacterial antigen and was not affected by deficiencies in the tumor necrosis factor receptors p55 or p75, the Fas receptor (CD95), or the respiratory burst enzymes or by forced expression of *bcl-2* in hematopoietic cells.

Upon encountering antigen, specific T cells proliferate and differentiate into effectors of varied types according to distinct signals in their environment. This expansion is usually followed by a contraction phase where T cells disappear as they undergo apoptosis and are thus eliminated, together with the removal of the antigenic challenge (1). In certain infectious diseases where the microbe resists killing by the immune system, this sequence of events may not always be present as antigenic stimulation persists for prolonged periods of time. Examples of such infections are found following invasion of the host by different mycobacterial genera, schistosoma, and human immunodeficiency virus. In those infections, microbial persistence is accompanied by immunopathological findings, including the development of necrosis, fibrosis, and lymphopenia.

T-cell loss has been observed during *Mycobacterium avium* infections. Using a disseminated model of *M. avium* infection induced by the intravenous inoculation of high numbers of viable mycobacteria, we reported that a highly virulent strain (ATCC 25291 with a smooth-transparent SmT morphotype) induced extensive T-cell depletion in the spleens of infected mice (9, 10). In contrast, a less virulent strain (*M. avium* 2447) did not (9). In a different model of infection initiated by exposure to an intratracheal infection, Cheers and colleagues dissected the development of severe anergy associated with pronounced T-cell loss at late stages of *M. avium* infection (13, 14, 24). In the latter studies, such T-cell loss was observed at different sites of infection and was explained by the increase in apoptosis of T cells in infected animals (14). More recently, it was shown to be mediated by CD95 in $CD4^+$ T cells and prevented by Bcl-2 in $CD8^+$ T cells (38). T-cell loss was also described during *Mycobacterium bovis* BCG infection by Dalton and coworkers (5). In their study, they were able to incriminate IFN-γ and nitric oxide (NO) as the culprits of such phenomenon. However, the role of IFN-γ and NO has not been analyzed in an in vivo model of T-cell loss, namely, during *M. avium* infections.

The mechanisms of T-cell depletion may vary according to each specific case. T cells may die by "neglect" due to lack of costimulation namely by deficient production of interleukin-2 (IL-2) and other cytokines or may die when certain death receptors are triggered (18). Among the latter one can find tumor necrosis factor (TNF) receptor superfamily (TNFRSF) members such as the TNF receptors (TNFR), TNF-related apoptosis-inducing ligand receptors, CD95/Fas, and death receptor 3 (23). Cytokines such as IL-10, IL-6, and transforming growth factor β1 (TGF-β1) have been found to inhibit T-cell death (2, 12, 34) whereas IFN-γ has been known for its death promoting activity (22). Free radicals may also lead to T-cell apoptosis (5, 19).

Here, we attempted to determine the mechanism by which T-cell loss occurred during infection with the virulent 25291 strain of *M. avium*. Our principal tool was a panel of gene-deficient animals wherein we determined the relationship between T-cell numbers, IFN-γ production, and susceptibility to infection by *M. avium*. Since IFN-γ has been suggested to be responsible for T-cell death in mycobacterial infections (5), we studied mice deficient in IFN-γ, mice deficient in a cytokine that regulates its production (IL-12) and mice deficient in the generation of reactive oxygen and nitrogen species, also known for their apoptosis-inducing activity (5, 19), given that IFN-γ primes phagocytes for the enhanced production of these molecules. Similarly, the known involvement of TNF-α in the apoptosis of T cells (23, 37) implicated this cytokine in T-cell depletion and we therefore studied mice deficient in this cytokine as well as mice deficient in the expression of its receptors. In order to identify specific apoptotic mechanisms in the T-cell depletion, we analyzed mice lacking the expression of the

* Corresponding author. Mailing address: Laboratory of Microbiology and Immunology of infection, Institute for Molecular and Cell Biology, University of Porto, Rua do Campo Alegre 823, 4150-180 Porto, Portugal. Phone: 351 226074952. Fax: 351 226099157. E-mail: rappelb@ibmc.up.pt.

TABLE 1. List of the strains used in this work to assess the role of individual molecules in the fate of infection and of T cells and brief descriptions of their phenotypes

Strain	Genetic defect[a]	Phenotype and rationale for use in this work (references)
B6.TNFRSF1a$^{-/-}$	TM of *tnfrsf*1a	Does not express type 1 (p55) TNF receptors involved in apoptosis, namely, of T cells (23)
B6.TNFRSF1b$^{-/-}$	TM of *tnfrsf*1b	Does not express type 2 (p75) TNF receptors
B6.TNF$^{-/-}$	TM of *tnfsf*2	Lacks production of TNF-α, which may induce apoptosis in many cell types, namely, of T cells (23, 37)
B6.MRL.*lpr*	SP of *tnfrsf*6	Does not express CD95/Fas, which is involved in apoptosis, namely, of T cells (23, 37)
B6.IFNγ$^{-/-}$	TM of *ifng*	Lacks production of IFN-γ, which activates macrophages and can lead to apoptosis of lymphocytes (5)
B6.IL12p40$^{-/-}$	TM of *il12*b	Lacks production of IL12p40, which activates T cells for IFN-γ secretion
B6.NOS2$^{-/-}$	TM of *nos2*	Lacks the inducible nitric oxide synthase, and macrophages do not produce NO involved in apoptosis, namely, of T cells (5)
B6.p47$^{phox-/-}$	TM of *ncf*1	Lacks the cytosolic 47-kDa component of phagocytes' NADPH oxidase (p47phox) and have deficient respiratory burst and consequently reduced apoptosis mediated by oxygen-free radicals (19)
C57B1/6$^{+/bcl2}$	TG of human *bcl*-2	Expression of human BCL-2 under the *vav* promoter leads to overexpression of BCL-2 in hematopoietic cells, causing inhibition of the mitochondrial pathways of apoptosis (16, 25)

[a] TM, targeted mutation; SP, spontaneous mutant; TG, expressing a transgene leading to the expression of a new gene product.

death receptor CD95/Fas (23, 37) and mice overexpressing the apoptosis-inhibiting protein BCL-2 (16). Our data incriminate IFN-γ as a mediator of the T-cell depletion.

MATERIALS AND METHODS

Mice. A complete listing of the mutant mice used in this study with a brief description of their phenotypes, justifying their use here, is shown in Table 1. Female C57BL/6J, B6.TNFRSF1a$^{-/-}$ (p55$^{-/-}$), B6.TNFRSF1b$^{-/-}$ (p75$^{-/-}$), B6.MRL.*lpr*, B6.IFN-γ$^{-/-}$, B6.IFN-γ-R$^{-/-}$, B6.IL12p40$^{-/-}$, and Rag-2$^{-/-}$ mice were purchased from the Jackson Laboratories (Bar Harbor, ME). Breeder mice for strain B6.TNF$^{-/-}$ were purchased from Bantin and Kingman Universal (North Humberside, United Kingdom). Progeny was obtained in our facilities. NOS2-deficient mice were bred in our facilities from a breeding pair kindly provided by J. D. MacMicking and C. Nathan (Cornell University, New York, NY) and J. Mudgett (Merck Research Laboratories, Rahway, NJ). NOS2-deficient mice in a C57BL/6 background (B6.NOS2$^{-/-}$) were obtained by backcrossing the original strain into a C57BL/6 background for seven generations. Transgenic mice overexpressing human BCL2 in the hematopoietic cell lineage (C57BL/6$^{+/bcl2}$) were kindly supplied by J. Adams (Walter and Eliza Hall Institute of Medical Research, Melbourne, Australia [25]). NADPH oxidase-deficient B6.p47$^{phox-/-}$ mice were a gift from S. Holland (National Institute of Allergy and Infectious Diseases, National Institutes of Health, Bethesda, MD). C57BL/6 mice engineered to express green fluorescent protein (GFP) (B6.GFP) (36) were crossed, at the Trudeau Institute, to transgenic mice that express the Vβ3/Vα11 T-cell receptor (TCR) that recognizes a pigeon cytochrome *c* peptide in the context of I-E^{k} (17). Mice were kept in high-efficiency particulate air filter-bearing cages and fed autoclaved chow (Harlan) and water. Female mice were used at 6 to 9 weeks of age.

Bacteria. *M. avium* strain 25291, exhibiting a smooth-transparent morphotype, was obtained from the American Type Culture Collection (Manassas, VA). Mycobacteria were grown in Middlebrook 7H9 medium (Difco, Detroit, MI) containing 0.04% Tween 80 (Sigma, St. Louis, MO) at 37°C until the mid-log phase of growth. Bacteria were harvested by centrifugation and resuspended in a small volume of saline containing 0.04% Tween 80. The bacterial suspension was briefly sonicated with a Branson sonifier (Danbury, CT) to disrupt bacterial clumps, diluted, and stored in aliquots at −70°C until used. Before inoculation, bacterial aliquots were thawed at 37°C and diluted in saline to the desired concentration.

In vivo infection. Female mice aged 6 to 9 weeks were infected intravenously with 10^6 CFU of *M. avium* strain 25291 through a lateral tail vein. Infected mice were sacrificed at different time points of infection, and the livers, spleens, and lungs were aseptically collected and homogenized in a 0.04% Tween 80 solution in distilled water. The number of CFU of *M. avium* in the organs of the infected mice was determined by serial dilution and plating of the tissue homogenates into Middlebrook 7H10 agar medium (Difco, Sparks, MD) supplemented with oleic acid-albumin-dextrose-catalase. The number of bacterial colonies was counted after culture for 2 weeks at 37°C. Statistical comparisons of the mycobacterial loads between deficient and control mice were performed using the Student's *t* test.

Cell preparation. A single-cell suspension was prepared from the spleen by passing the organ through a 70-μm nylon cell strainer and lysing the red blood cells by using Gey's solution (29). Lung cell suspensions were prepared by perfusing cold saline containing heparin through the heart. Once lungs appeared white, they were removed and sectioned in ice-cold medium using sterile razor blades. Dissected lung tissue was then incubated in Collagenase IX (0.7 mg/ml; Sigma) and DNase (30 μg/ml; Sigma) at 37°C for 30 min (29). Digested lung tissue was gently disrupted by passage through a 70-μm nylon cell strainer, and the resultant single-cell suspension was treated with Gey's solution to remove any residual red blood cells, washed twice, and counted. Cells prepared in this way were used for flow cytometric analyses.

Detection of IFN-γ. Single-cell suspensions from the spleens of each of the infected mice were prepared by teasing portions of the spleen with forceps in Dulbecco's modified Eagle tissue culture medium (DMEM; Life Technologies, Paisley, United Kingdom) supplemented with 10% fetal calf serum (FCS; Life Technologies). Erythrocytes were lysed by incubation of the cell suspensions with hemolytic buffer (155 mM NH_4Cl, 10 mM KHCO3, pH 7.2) for 5 min at room temperature. The cell suspensions were then thoroughly washed with Hanks' balanced salt solution (HBSS; Life Technologies) and resuspended in DMEM with 10% FCS. Cells were cultivated at a density of 2×10^5 cells/well in a U-bottom 96-well microtiter plate. Cells were incubated in triplicate in DMEM with 10% FCS with no further stimulus or in the presence of mycobacterial envelope proteins (4 μg/ml). Supernatants from the cultures were collected after 96 h of culture, and the IFN-γ produced was quantified by a two-site sandwich enzyme-linked immunosorbent assay (ELISA) method using anti-IFN-γ-specific affinity-purified monoclonal antibodies (R4-6A2 as capture and biotinylated AN-18 as detecting antibody) and a standard curve generated with known amounts of recombinant murine IFN-γ (Genzyme, Cambridge, CA). The sensitivity of the assay was 30 pg/ml. Serum from infected mice was obtained after allowing the blood to clot, and IFN-γ titers were determined as described previously. Mycobacterial envelope proteins were prepared from *M. avium* strain 25291 grown in Sauton medium as described elsewhere (26).

Flow cytometry. For the immunofluorescence staining, 10^6 cells were incubated in a 96-well microtiter plate with fluorescein isothiocyanate (FITC)-conjugated anti-CD4 antibody (dilution, 1:100) and phycoerythrin (PE)-conjugated anti-CD8 antibody (dilution, 1:100) or FITC-conjugated anti-CD19 antibody (dilution, 1:100) and PE-conjugated anti-MAC-1 antibody (dilution, 1:100) in phosphate-buffered saline (PBS) containing 3% FCS. All antibodies were from BD Pharmingen (San Diego, CA). The cells were washed twice with PBS containing 3% FCS, and propidium iodide (Sigma, St. Louis, MO) was added to the cells at a final concentration of 1 μg/ml to allow the exclusion of dead cells. The analysis of the cell populations was based on the acquisition of 10,000 events in a Becton Dickinson FACSort instrument equipped with CellQuest software. Alternatively, single-cell suspensions of cells were stained with labeled antibodies specific for CD4 (allophyocyanin-labeled clone GK1.5), CD3 (peridinin chlorophyll protein [PerCP]-labeled clone 145-2C11), and CD44 (FITC-labeled clone IM7). Cells were then fixed and permeabilized, and the presence of intranuclear BrdU was determined using a (PE)-labeled antibody (BrdU flow kit; Becton Dickinson). Cells were analyzed using CellQuest on a Becton Dickinson FACSCalibur dual-laser flow cytometer with excitation at 488 nM and 633 nM. Lymphocytes were gated based on their forward and side-scatter characteristics and then on CD4 and CD3, and the numbers of such lymphocytes per organ were determined. CD4-positive lymphocytes were then analyzed for their expression of BrdU, and this frequency was applied to the total number of CD4 T cells per organ to determine the number of recently proliferated cells per organ. For the analysis of apoptotic cells, a total of 5×10^5 splenic cells were incubated in a

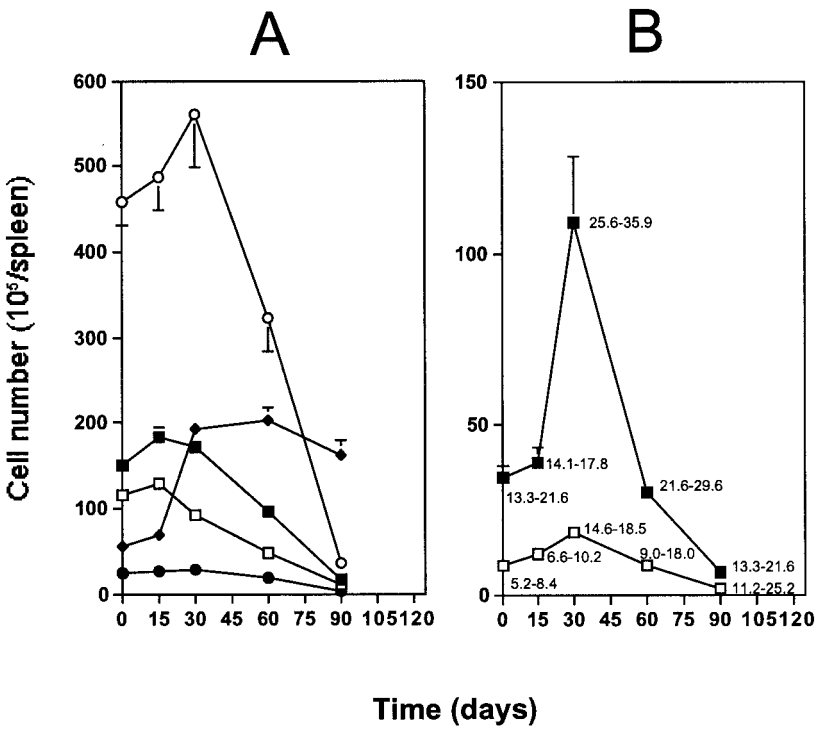

FIG. 1. Cellular composition in the spleens of C57BL/6 mice infected with 10^6 CFU of *M. avium* 25291. (A) Total number of $CD19^+$ (open circles), $Mac1^+$ (diamonds), $CD4^+$ (closed squares), $CD8^+$ (open squares), and $DX5^+$ (closed circles) cells; (B) total number of annexin V^+ 7-AAD^- cells gated on $CD4^+$ (closed squares) or $CD8^+$ (open squares) cells. The values indicated near each symbol indicate the range of percentages of annexin V^+ 7-AAD^- cells among each population.

96-well microtiter plate with either PE-conjugated anti-CD4 antibody or PE-conjugated anti-CD8 antibody (Pharmingen) at a dilution of 1:100 in PBS containing 3% FCS for 30 min. The cells were washed twice with PBS–3% FCS and a third time with binding buffer (10 mM HEPES buffer containing 0.14 mM NaCl and 2.5 mM $CaCl_2$, pH 7.4) and incubated in 100 μl binding buffer containing 5 μl of FITC-conjugated annexin V (Pharmingen) and 4 μl of 7-AAD (Pharmingen) for 15 min at room temperature in the dark. The stained cell suspensions were then diluted in binding buffer to a final volume of 0.5 ml and immediately analyzed.

BrdU incorporation assay. C57BL/6 and B6.IFN-$\gamma^{-/-}$ were intravenously infected with 10^5 *M. avium* 25291. At specific times postinfection, mice were given 1 μg of the nucleotide analog bromodeoxyuridine (BrdU) via the intraperitoneal route. Twenty-four hours post-BrdU delivery, mice were euthanized and the lungs and spleens harvested.

Chimerization of Rag-deficient mice. Spleen cells were isolated from control C57BL/6 mice or from mutant mice and incubated for 2 h in a nylon wool column (1.2 g per 10-ml column) in DMEM containing 2% FCS. Nonadherent cells were recovered by gently washing the columns with 20 ml of warmed culture medium. This T-cell-enriched population of spleen cells (routinely, a purification of 80% CD3-positive cells was obtained) was washed and intravenously transfused into Rag1$^{-/-}$ mice (one spleen cell equivalent per mouse, around 20×10^6 cells). Recipient mice were allowed to repopulate the lymphoid organs for 3 weeks (30) before we infected them with *M. avium*.

Adoptive transfer of GFP-expressing T cells. Naïve CD4 T cells were isolated from mice expressing a pigeon cytochrome *c* peptide-specific TCR transgene and a GFP transgene and cultured with peptide antigen and cytokines to generate Th1 effector CD4 T cells as previously described (17). Briefly, $CD4^+$ T cells were cultured with the DCEK-ICAM fibroblast cell line (I-E^{k+}, B7.1$^+$, B7.2$^+$, and ICAM-1$^+$) at a 2:1 ratio (CD4:antigen-presenting cell) in the presence of the pigeon cytochrome *c* peptide fragment from amino acids 88 through 104 as the antigen at a dose of 5 μM and with exogenously added IL-2 (80 U/ml), IL-12 (2 ng/ml), and anti-IL-4 (10 μg/ml). Four-day in vitro-derived $CD4^+$ T-cell effectors were then transferred into either C57BL/6 or B6.IFN-$\gamma^{-/-}$ mice infected 30 days previously with 10^5 *M. avium* 25291 or uninfected C57BL/6 mice or B6.IFN-$\gamma^{-/-}$ mice (10^7 cells per mouse). Four days following transfer, the host mice were euthanized and single-cell suspensions of the lung and spleen were prepared and analyzed by flow cytometry. Cells were gated on the expression of the GFP and then analyzed for the expression of CD4 and CD44 or for expression of the annexin-V ligand and ability to exclude 7-AAD

Statistical analysis. Data were compared by using Student's *t* test for paired data and the analysis of variance test.

RESULTS

T-cell loss during infection of C57BL/6 mice with *M. avium* 25291, a highly virulent strain. When C57BL/6 mice are intravenously infected with high doses (10^6 CFU) of the virulent *M. avium* strain ATCC 25291, there is a progressive uncontrolled infection despite the emergence of an immune response characterized by prominent production of IFN-γ and extensive macrophage activation (9). Concomitant with this uncontrolled bacterial growth, progressive loss of T and B lymphocytes and accumulation of macrophages can be detected in the spleen (Fig. 1A). That the progressive loss of T lymphocytes may be mediated by apoptosis was indicated by an increased frequency of these cells that were positive for the surface expression of phosphatidylserine, as determined by annexin V staining (Fig. 1B). The number of annexin V-positive $CD4^+$ cells was particularly high and peaked at day 30. From day 30 onwards, the absolute number of apoptotic T cells dropped as a function of the reduced number of lymphocytes within the spleen; however, the frequency of annexin V-positive cells within the T-cell population remained above normal values (numbers beside each point in Fig. 1B) until day 60 of infection, becoming similar to control values at day 90, when very few viable cells remained.

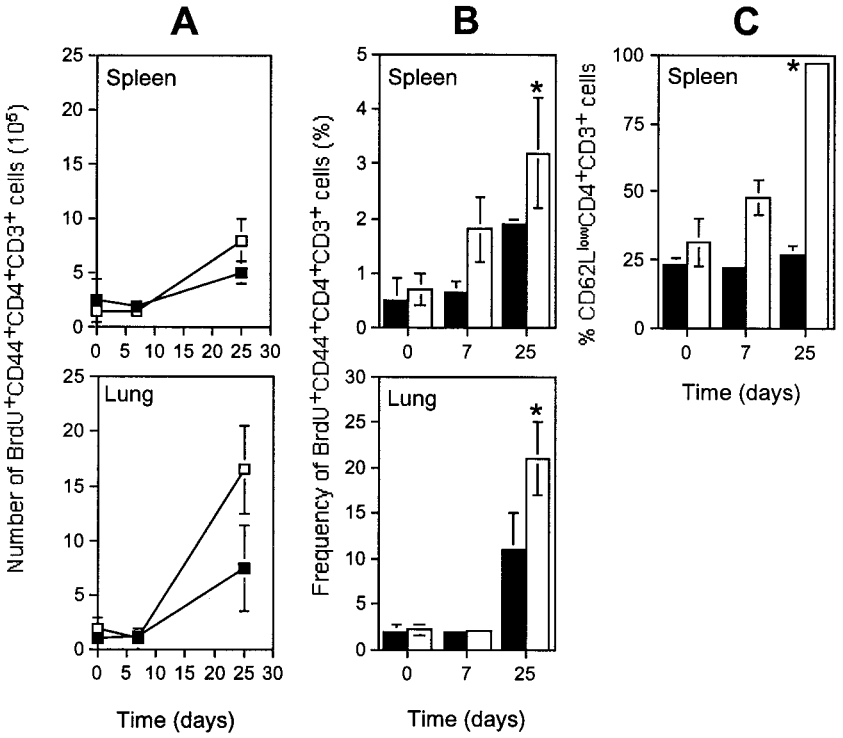

FIG. 2. IFN-γ restricts T-cell proliferation during infection. C57BL/6 (closed symbols and columns) and B6.IFN-$\gamma^{-/-}$ (open symbols and columns) mice were intravenously infected with 10^5 *M. avium*. At specific times postinfection, mice were euthanized and lungs and spleens harvested. Twenty-four hours prior to harvest, mice had been treated with 1 μg of BrdU intraperitoneally. Tissues were processed for flow cytometric analysis and BrdU labeling. Number (A) and frequency (B) of recently proliferated ($BrdU^+$) activated ($CD44^+$) $CD4^+$ T cells were studied in the spleen and lung. The frequency of activated ($CD62L^{low}$) $CD4^+$ T cells was also studied in the spleen (C). Data points show means of values derived from four individual mice at all time points (*, $P \leq 0.05$).

Role of IFN-γ production in T-cell survival. Dalton et al. (5) have shown that during BCG infection, IFN-γ leads to the contraction of the T-cell response through the induction of apoptosis of T cells and that such a phenomenon is mediated by nitric oxide. To determine whether and how IFN-γ mediates T-cell depletion in our model, we compared the T-cell response in *M. avium*-infected B6 and B6.IFN-$\gamma^{-/-}$ mice. In a first analysis, we measured the ability of T cells to incorporate BrdU as a measure of T-cell proliferation. As shown in Fig. 2A and B, IFN-γ-deficient mice showed increased accumulation of recently proliferated T cells in response to the infection compared to control C57BL/6 mice. This accumulation was seen in both the spleen and the lung. The increased proliferation was evident as an increase in the total number of BrdU-positive, activated ($CD44^+$) T cells (not statistically significant) as well as an increase in their frequency (statistically significant at day 25 of infection). It also appeared that activated effector $CD4^+$ T cells, defined by reduced expression of the CD62L selectin, were more able to accumulate in the absence of IFN-γ (Fig. 2C).

IFN-γ-deficient mice were as susceptible to bacterial growth as control mice but failed to show the same profile of T-cell depletion seen in the control mice. Specifically, the IFN-γ-deficient mice exhibited a pronounced expansion of T cells, followed by an eventual contraction in the late stages of infection (Fig. 3A). Even though this contraction occurred, unlike the control animals, where profound depletion was seen, T-cell numbers never declined below the levels found in uninfected animals. Similar data were obtained with IL-12p40$^{-/-}$ mice (Fig. 3A), which had severely impaired IFN-γ responses (no cytokine was detectable in their serum or culture supernatants). In contrast, IFN-γ responses in NOS2$^{-/-}$ mice were enhanced compared to wild-type mice both in the serum (7.9-fold at day 30; $P < 0.05$) and upon in vitro stimulation (4.6-fold at day 30 and 2.4-fold at day 60; $P < 0.05$) and T-cell loss was undistinguishable from that in control mice (Fig. 3A). Again, in contrast to any other mouse investigated, the NOS2$^{-/-}$ mice were able to control mycobacterial proliferation and maintained a prolonged bacteriostasis lasting up to 4 months of infection (Fig. 3A and data not shown), confirming previous work from our group (15).

To determine whether the cellular source of IFN-γ was important for the depletion of T cells to occur, we prepared chimerized Rag-deficient mice harboring T cells from either C57BL/6 or B6.IFN-$\gamma^{-/-}$ mice. When these chimeric mice were infected, T-cell depletion was significantly more extensive in the B6 chimeras but still occurred in the B6.IFN-$\gamma^{-/-}$ chimeras (Fig. 3B), although in the latter case, differences were statistically significant for only $CD8^+$ T cells. To assess whether IFN-γ acted directly on T cells to induce apoptosis or through the action of other cell types, we chimerized Rag$^{-/-}$ mice with T cells lacking the IFN-γ receptor (i.e., from B6.IFN-γ-R$^{-/-}$ mice). As shown in Fig. 3C, IFN-γ-R-deficient T cells were depleted to a level equivalent to that of IFN-γ-responsive T cells.

The observation that the majority of T cells (and B cells) are

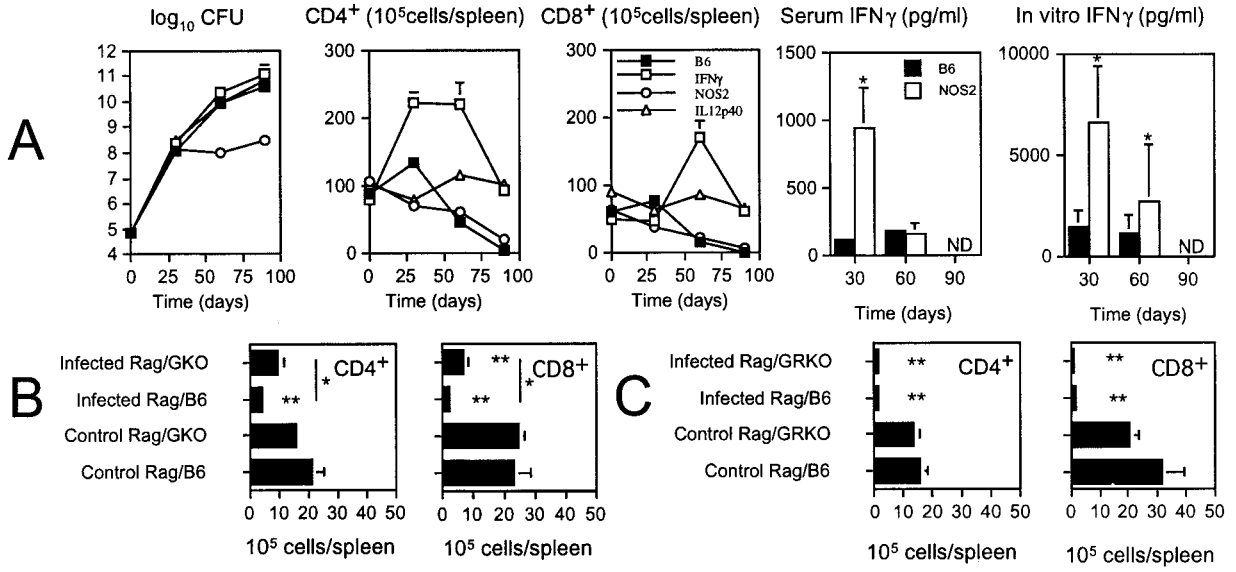

FIG. 3. Role of IFN-γ in infection-induced T-cell depletion. (A) Growth of *M. avium* ATCC 25291 in the spleen; number of splenic T cells in C57BL/6 (closed squares), B6.IFN-$\gamma^{-/-}$ (open squares), B6.IL12p40$^{-/-}$ (triangles), and B6.NOS2$^{-/-}$ (circles) mice; and IFN-γ concentrations in the serum and culture supernatants of B6 (closed columns) and B6.NOS2$^{-/-}$ (open columns) mice. No IFN-γ was detectable in the samples from the B6.IFN-$\gamma^{-/-}$ or B6.IL12p40$^{-/-}$ mice. Results were confirmed in an independent experiment. (B) T-lymphocyte depletion in Rag$^{-/-}$ mice that received T-cell-enriched spleen cells from either C57BL/6 (Rag/B6) or B6.IFN-$\gamma^{-/-}$ (Rag/GKO) mice 3 weeks before they were intravenously infected with 10^6 CFU of *M. avium* 25291. Spleen cell populations were evaluated at 90 days of infection. Data represent the means of five mice per group in one experiment. Statistically significant differences between infected and noninfected mice are labeled ** ($P < 0.01$), whereas differences between infected B6 chimeras (Rag/B6) and B6.IFN-$\gamma^{-/-}$ chimeras (Rag/GKO) are labeled * ($P < 0.05$). (C) T-lymphocyte depletion in Rag$^{-/-}$ mice that received T-cell-enriched spleen cells from either C57BL/6 (Rag/B6) or B6.IFN-γ-R$^{-/-}$ (Rag/GRKO) mice 3 weeks before they were intravenously infected with 10^6 CFU of *M. avium* 25291. Spleen cell populations were evaluated at 90 days of infection. Data represent the means of five mice per group in one experiment, and statistically significant differences between infected and noninfected mice are labeled ** ($P < 0.01$). ND, not done.

lost suggests that depletion of these cells is indiscriminate. To confirm this was the case, we transferred CD4$^+$ TCR effector cells specific for a non-*M. avium* antigen and which express GFP as a detectable tracer either into *M. avium*-infected C57BL/6 or B6.IFN-$\gamma^{-/-}$ mice or into uninfected controls and evaluated the survival of the transferred cells in the recipient host. As shown in Fig. 4A, the transferred cells were less able to persist in the spleens of infected mice than were those in the spleens of noninfected hosts. This enhanced loss correlated well with increased levels of apoptosis among the T cells (Fig. 4B). Furthermore, the induction of apoptosis among the transferred cells was more extensive when the cells were administered to C57BL/6 mice than when they were given to IFN-γ-deficient animals (Fig. 4C), when evaluated in the spleens of recipient mice.

IFN-γ appears from this data to be an indirect inducer of T-cell loss during *M. avium* infection; however, nitric oxide does not appear to be the responsible effector molecule. To

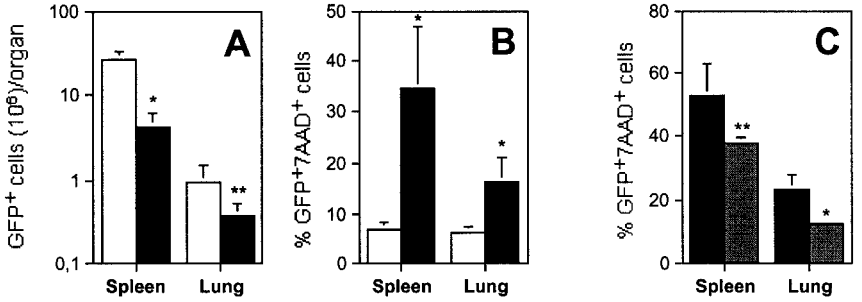

FIG. 4. T cells are lost nonspecifically during infection. Splenocytes from uninfected B6.GFP mice were harvested and treated ex vivo to generate effector cells. These pigeon cytochrome *c*-specific GFP effector cells were then transferred into non-GFP mice either that were uninfected (open bars) or which had been infected 30 days previously (black bars). On day 4 posttransfer, recipient mice were euthanized and the number of transferred GFP cells remaining in the spleen and lung was determined by flow cytometry (A) (*, $P \leq 0.002$; **, $P = 0.065$). The percentage of apoptotic GFP-positive cells was also determined by flow cytometry (B) (*, $P \leq 0.002$). In an independent experiment, GFP CD4$^+$ effector T cells were transferred into *M. avium*-infected C57BL/6 (closed columns) or B6.IFN-$\gamma^{-/-}$ (gray columns) mice and the frequency of apoptotic cells was determined 4 days later (C) (*, $P = 0.07$; **, $P = 0.02$). Two independent experiments were performed. Data represent means ± standard deviations, with $n = 4$ (experiment 1) or $n = 3$ (experiment 2).

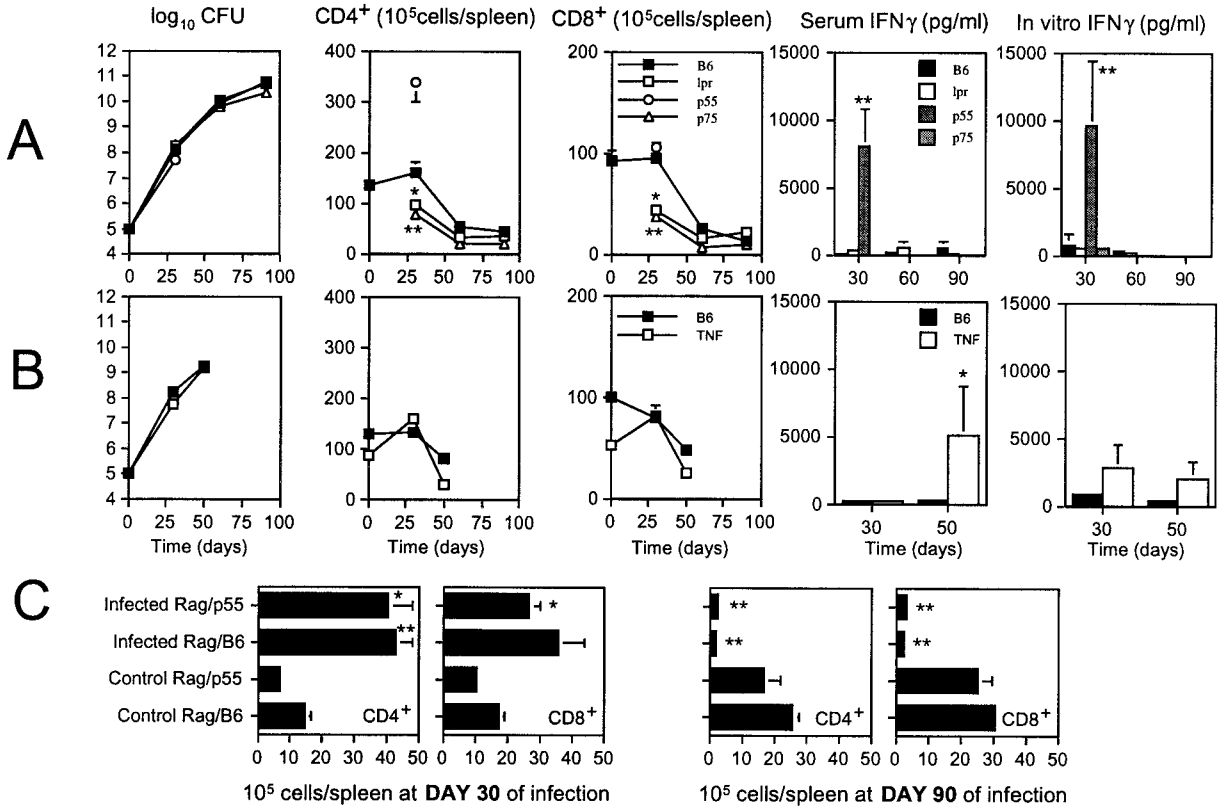

FIG. 5. TNFR superfamily death receptors are not required for infection-induced T-cell death. (A) Growth of *M. avium* ATCC 25291 in the spleen; number of splenic T cells in C57BL/6 (closed squares), B6.MRL.*lpr* (open squares), B6.TNFRSF1a/p55$^{-/-}$ (circles), and B6.TNFRSF1b/p75$^{-/-}$ (triangles) mice; and IFN-γ concentrations in the serum and culture supernatants of B6 (closed columns), B6.MRL.*lpr* (open columns), B6.TNFRSF1a/p55$^{-/-}$ (dark gray columns), and B6.TNFRSF1b/p75$^{-/-}$ (light gray columns) mice. Statistically significant differences between mutant and B6 mice are labeled * ($P < 0.05$) or ** ($P < 0.01$). (B) T-lymphocyte depletion in TNF-deficient mice: C57BL/6 and B6.TNF$^{-/-}$ mice were intravenously infected with 10^6 CFU of *M. avium* 25291, and spleen cell populations and bacterial loads were evaluated at the indicated time points; IFN-γ concentrations were evaluated in the serum and culture supernatants for B6 (closed columns) and B6.TNF$^{-/-}$ (open columns) mice. Statistically significant differences between mutant and B6 mice are labeled * ($P < 0.05$). (C) T-lymphocyte depletion in chimeric Rag$^{-/-}$ mice: Rag$^{-/-}$ mice that received T-cell-enriched spleen cells from either C57BL/6 or B6.TNFRp55$^{-/-}$ mice 3 weeks earlier were intravenously infected with 10^6 CFU of *M. avium* 25291, and spleen cell populations were evaluated at the indicated time points. Statistically significant differences between infected and noninfected mice are labeled * ($P < 0.05$) or ** ($P < 0.01$). Data represent the means of five mice per group in one experiment.

investigate the mechanism further, we continued to test additional candidate molecules directly involved in T-cell demise.

Analysis of mice with the mutated forms of selected TNFR superfamily members. Given that several of the TNFR superfamily molecules are involved in the induction of apoptosis of T cells, we investigated whether specific members of this family were involved in the T-cell depletion seen here. Mice deficient in CD95/Fas (TNFRSF-6), the *lpr* mice, or mice with engineered mutations in either the type 1 (p55) or the type 2 (p75) receptors for TNF (TNFRSF 1A and 1B) were therefore infected and the cellular response examined. T-cell loss in both the *lpr* and p75$^{-/-}$ mice was observed to occur even at levels superior to those of wild-type mice (Fig. 5A). Thus, T-cell numbers at day 30 of infection were smaller in those mutant mice than in C57BL/6 animals ($P < 0.01$ in p75$^{-/-}$ mice; $P < 0.05$ in *lpr* mice). In contrast to the B6 profile, the p55$^{-/-}$ mice exhibited a marked CD4$^+$ T-cell expansion (Fig. 5A) during the first month. However, these mice succumbed to infection by day 40 of infection, as previously reported by Ehlers et al. (6), and further analysis of the cellular response could not be performed. These mice appeared to be mounting a type 1 response, as indicated by high serum levels of IFN-γ (42-fold higher in p55$^{-/-}$ mice than in C57BL/6 mice; $P < 0.001$) and a high antigen-specific IFN-γ response by splenocytes (12-fold higher than C57BL/6, $P < 0.001$) (Fig. 5A). The p75$^{-/-}$ and *lpr* mice had IFN-γ serum levels and antigen-specific responses similar to those of C57BL/6 mice (Fig. 5A). The susceptibility of *lpr* and p75$^{-/-}$ mice to infection was similar to that of wild-type mice throughout the 3 months of infection studied (Fig. 5A). No conclusive analysis could be made from the p55$^{-/-}$ mice as they succumbed early in infection, although a trend for a reduction in mycobacterial loads was apparent on day 30 of infection.

The fact that the p55-deficient mice exhibited a pronounced type 1 cellular response implicated TNF as a potential regulator of T-cell function. To investigate the role of TNF in T-cell loss, we infected mice deficient in this cytokine. As was seen in the p55$^{-/-}$ mice, the TNF$^{-/-}$ mice had a reduction in survival during infection (mean survival time, 57.5 ± 8.4 days; $n = 19$ mice). These animals were studied until day 50 of infection,

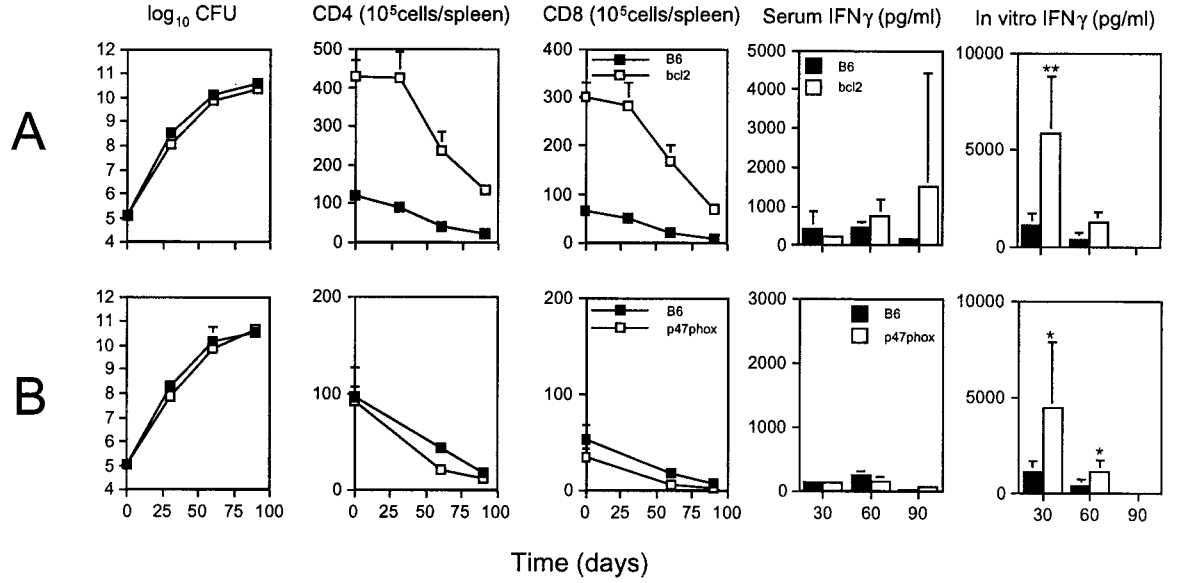

FIG. 6. Growth of *M. avium* ATCC 25291 in the spleen, number of splenic T cells, and IFN-γ concentrations in serum and culture supernatants in mice with different immunological deficiencies. (A) C57BL/6 (closed squares and columns) and C57BL/6.tgBcl2 (open squares and columns) mice; (B) C57BL/6 (closed squares and columns) and B6.p47$^{phox-/-}$ (open squares and columns) mice. Each group of graphs represents an independent experiment using five mice per group and per time point. Results were confirmed in an independent experiment. Statistical differences in IFN-γ production between the two mouse strains were labeled * ($P < 0.05$) or ** ($P < 0.001$).

showing no T-cell expansion at day 30 and exhibiting the same type of T-cell loss at the last time point studied as that observed in wild-type controls infected in parallel (Fig. 5B). These mice were able to generate higher levels of IFN-γ in serum, although the antigen-specific response was only marginally improved over the control mice (Fig. 5B). While these data implicated TNF in the modulation of serum IFN-γ, TNF does not seem to be mediating the T-cell depletion seen in this model. To further investigate if p55 may mediate T-cell depletion, we chimerized T-cell-deficient Rag$^{-/-}$ mice with T cells from either C57BL/6 or B6.p55$^{-/-}$ mice and determined the extent of T-cell depletion upon *M. avium* infection. These chimeras survived up to day 90 of infection and, as can be seen in Fig. 5C, lymphocytes lacking the p55 molecule were as susceptible to depletion as were intact lymphocytes. Thus, neither TNF nor p55 is required for T-cell loss during *M. avium* infection.

***Bcl-2* overexpression does not prevent T-cell loss during *M. avium* infection.** Our data implicate an apoptotic process in the observed T-cell depletion, and we thus decided to investigate the ability of antiapoptotic molecules in preventing this depletion. Apoptosis that is initiated by caspase 9 following leakage of cytochrome *c* from the mitochondria can be inhibited by BCL2, a mitochondrial protein (16). Mice engineered to overexpress human *bcl-2* in hematopoietic cells have lymphocytes which are protected from certain forms of apoptosis (16). These mice provided us with a tool to determine whether T-cell depletion was progressing through the cytochrome *c*/caspase 9 pathway. We therefore infected these mice and analyzed the T-cell response. Although the transgenic animals had higher numbers of T cells at the beginning of infection, they underwent the same level of T-cell depletion seen in the control mice (Fig. 6A). Thus, at 90 days of infection, CD4$^+$ T cells were reduced 66.6% in transgenic animals compared to 78.2% in C57BL/6 mice and CD8$^+$ T cells were reduced 84.8% in transgenic animals compared to 84.5% in C57BL/6 mice. Although *bcl-2* transgenic mice had IFN-γ serum levels similar to those of C57BL/6 mice (Fig. 6A), spleen cells from *bcl-2* transgenic mice showed an increased ability to secrete IFN-γ upon antigenic stimulation compared to the control cells (fivefold at day 30 of infection; $P < 0.001$) (Fig. 6A). Absolute numbers of IFN-γ-producing T cells, as evaluated by the ELISpot assay, remained proportionally higher in infected *bcl-2* transgenic mice compared to C57BL/6 controls (data not shown). This increase in IFN-γ did not alter the progression of bacterial growth (Fig. 6A). It would thus appear that the apoptosis seen in this model does not use the cytochrome *c*/caspase 9 (mitochondrial) pathway.

Reactive oxygen species are not responsible for the T-cell loss. An alternative process whereby apoptosis can occur is via products from the respiratory burst. The production of these oxygen-free radicals is also enhanced in IFN-γ-activated phagocytes. To determine whether products of the respiratory burst were mediating the T-cell depletion in this model, we infected mice deficient in the p47 chain of the NADPH oxidase (p47$^{phox-/-}$ mice) and monitored the cellular response. As shown in Fig. 6B, p47$^{phox-/-}$ mice showed similar T-cell loss during infection while serum IFN-γ was within the range of concentrations found in the control animals (Fig. 6B). Antigen-specific responses in vitro were however higher in the deficient mouse (3.9-fold at day 30 and 2.6-fold at day 60; $P < 0.05$), but this had no impact on bacterial growth (Fig. 6B).

DISCUSSION

We have used a highly virulent strain of *M. avium* to address the role of different immune mediators in the loss of T cells occurring during infection. The growth of this strain is not

controlled in susceptible mice despite the emergence of an immune response known to be protective against other less virulent strains (9). Thus, since this strain resists the antimycobacterial mechanisms induced during the immune response, it is a suitable model to analyze the role in such T-cell depletion of immune mediators like IFN-γ which play a protective role against other mycobacteria without any interference on the course of the infection. We found that T cells underwent apoptosis at accelerated rates after the initial month of infection. This was similar to the results previously reported by the group of Cheers and colleagues (14), although given the higher virulence of the mycobacterial strain, the phenomenon occurred with more rapid kinetics in our model. Our data extend the observations by this group by revealing the role of IFN-γ in the antigen-nonspecific elimination of these T cells and excluding classic mechanisms of T-cell apoptosis such as those mediated by TNF, NO, or Fas/CD95.

IFN-γ has been shown to lead to enhanced T-cell apoptosis in mycobacterial infections and to down-regulate the immune response to mycobacteria (3, 5, 27). Our data further highlight the role of IFN-γ in limiting the immune response to mycobacteria, namely, by promoting T-cell apoptosis and depletion. However, given the virulence of the *M. avium* strain used, the consequences were dramatically severe with a depletion of T cells up to 99% of the normal number as determined in the spleen. In this study, we showed that T-cell loss does not occur in IFN-γ-deficient animals when infected with *M. avium* and that these animals show increased rates of lymphocyte proliferation. The IFN-γ leading to T-cell depletion was produced by the T cells themselves but also had a T-cell-independent origin since chimeric mice with normal innate immunity and a T-cell compartment deficient in its ability to secrete IFN-γ still showed marked $CD8^+$ T-cell depletion. The depletion of $CD4^+$ T cells in these chimeras did not however reach statistical significance, raising the possibility that different subsets of T cells may differ in their threshold for IFN-γ-induced demise. The nature of the non-T-cell population secreting IFN-γ was not analyzed here, but we have previously shown that significant amounts of IFN-γ can be produced by cells expressing NK cell markers, in particular, Thy1 and DX5, during *M. avium* infection (8). Thus, it is likely that NK cells regulate the expansion of T cells as well as their elimination through the secretion of IFN-γ. Although IFN-γ was required for the loss of T cells, the increased production of this cytokine in some of the mutant strains did not apparently accelerate the rate of disappearance of the T cells.

In contrast to the report by Dalton et al. (5), we did not find nitric oxide required for T-cell depletion. The reason for this discrepancy most likely lies in the fact that we analyzed the role of this reactive species in vivo whereas the former work used an in vitro system to determine its role in T-cell apoptosis. Additionally, there might be differences associated with the mycobacterial species used, since the study by Dalton et al. focused on BCG. IFN-γ may directly induce T-cell death by promoting the synthesis of caspase 8 in the T cells (28), but in our system, IFN-γ most likely acts indirectly by activating other cell types, namely macrophages, which by themselves trigger T-cell death. This was established using chimeric mice that possessed T cells lacking the receptor for IFN-γ. However, the pathway triggered and the receptors involved remain to be identified. TNF signaling was not required for the induction of T-cell loss, although signaling through the type 1 TNF receptor may be involved in the restriction of $CD4^+$ T-cell expansion early in infection (Fig. 5). Since mice deficient in the type 1 TNF receptor (6) or TNF itself (data shown here and our unpublished observations) die prematurely from infection by *M. avium*, addressing the role of TNF and its type 1 receptor in these animals is not feasible since T-cell loss normally occurs after day 30 of infection in B6 animals. Therefore, we used chimerized Rag-deficient mice harboring T cells defective in the expression of type 1 TNF receptors and showed that TNF signaling was not required for the extensive loss of T cells. Mice deficient in the type 2 TNF receptor survived the infection long enough to allow similar analysis and to show that signaling through that receptor is also not required for the observed T-cell loss. We also showed that oxygen radicals produced through the respiratory burst in phagocytes, a pathway activated by the action of IFN-γ in these cells, are not required for the demise of T cells.

The fact that overexpression of functionally active human Bcl-2 did not prevent the loss of T cells would argue that T-cell death occurs through a mitochondrial-independent pathway, namely, through the triggering of surface-associated death receptors. Yet, we were able to exclude the involvement of either CD95/Fas and the type 1 TNF receptor, two molecules containing death domains and known to trigger apoptosis in T cells. There remain other possible candidates that should be investigated for their participation in this process of T-cell elimination, such as the receptors for TNF-related apoptosis-inducing ligand. These data contrast with recent results reported by Zhong et al. (38), who showed that apoptosis of $CD4^+$ T cells during infection by *M. avium* was dependent on CD95/Fas and that of $CD8^+$ T cells was prevented by overexpression of Bcl-2. The course of infection studied by the latter group is however distinct from the one we studied. Whereas infection by strain 25291 leads to T-cell depletion as early as the second month of infection, the apoptosis studied by Zhong and colleagues was evaluated at 16 weeks of infection. Differences in the kinetics of the infection may therefore result in the triggering of different pathways of T-cell elimination. Although we have studied only Bcl-2 for reasons related to availability of an animal model, it should be stressed that apoptosis pathways involving the mitochondria are regulated by additional members of the BCL family.

The mechanism leading to T-cell depletion in our system was antigen nonspecific in nature, since activated transgenic TCR-expressing T cells with an irrelevant specificity were eliminated at increased rates in infected animals compared to uninfected controls. Furthermore, this elimination was reduced when the transfer was done into IFN-γ-deficient mice compared to control C57BL/6 animals. The requirement for prior T-cell activation was not assessed, but given the extensive depletion occurring during infection, it is likely that both activated and naïve cells may undergo apoptosis. Alternatively, bystander activation could lead to T-cell activation just preceding their death. Our data provide evidence of extensive peripheral depletion of the T cells, namely, by showing increased apoptosis of endogenous T cells or of adoptively transferred effector T cells. However, additional mechanisms could influence and worsen the loss of T cells such as decreased

thymic output of new cells related either to thymic deficiencies or to decreased myelopoiesis. We have observed marked invasion of the bone marrow by infected macrophages, and mice do develop anemia at late stages of the infection (unpublished data). Also, we have observed thymic atrophy in mice infected by this *M. avium* strain (9). The relative contribution of these factors is presently being assessed in our laboratories.

In the present experiments, we found that resistance to the infection with *M. avium* was not affected by relatively large variations in the secretion of IFN-γ such as those observed among *bcl-2* transgenic mice. This is consistent with prior observations in other models where we found that increasing IFN-γ secretion by treatment with recombinant IL-12 or blocking of the IL-10 receptor did not increase protection against infection (31–33). Also, low T-cell numbers appear not to be the reason of the susceptibility to this highly virulent strain of *M. avium*, since *bcl-2* transgenic animals had increased T-cell numbers throughout the course of the infection, namely, those that produce IFN-γ and yet were as permissive to *M. avium* 25291 growth as the control mice.

The only instance where control of mycobacterial proliferation was achieved was with $NOS2^{-/-}$ mice. Not only was *M. avium* 25291 found to be resistant to NO as previously described by us (15), but NO was required for the mycobacteria to proliferate in the host. The basis for this phenomenon is yet unknown, but NO might affect the emergence of some unidentified protective mechanism, although the increase in T-cell numbers or IFN-γ responses by themselves cannot account for the observed resistance of $NOS2^{-/-}$ mice. A role in granuloma development has also been described by Ehlers et al. (7) who, however, did not find any difference in bacterial loads following treatment with a chemical inhibitor of NO synthase. Residual amounts of NO produced after chemical inhibition may justify this difference between the two models. Another alternative explanation is that *M. avium* may utilize NO in its metabolism in the macrophage after the emergence of the immune response, namely when hypoxic conditions set in inside the granulomas. We are currently pursuing studies in order to clarify the latter possibility.

Although we focused our study on T cells, the ones involved in protective immunity, extensive B-cell death also occurred during infection by the virulent *M. avium* strain used. Whether such B-cell depletion involves similar mechanisms remains to be determined.

The final mechanism of IFN-γ-mediated T-cell depletion remains to be uncovered. New information has shown that this cytokine may increase the expression of caspases in different cell types (4, 11, 20, 28, 35). This would make them more prone to undergo apoptosis by one of many different apoptotic stimuli. However, we saw that T cells unable to directly respond to IFN-γ are still susceptible to infection-induced death. These data have important implications not only in the context of mycobacterial infections but also to understand other infections where T-cell demise occurs at increased rates as a consequence of intense immune activation. In human tuberculosis, an association between increased apoptosis and IFN-γ secretion in the lesions has been described (20), suggesting that the phenomenon described here as a generalized one may also occur in a more discrete and localized infection. Showing that a cytokine which is pivotal in the expression of protective immunity may in addition promote susceptibility by leading to the elimination of T cells is a finding of great biological significance since the balance between the levels of IFN-γ needed for the control of the pathogen and those sufficient for the demise of T cells may determine the fate of the infection. Finally, there are also implications in the design of vaccines which are frequently screened based on their ability to induce strong IFN-γ responses. In this regard, we have shown that IFN-γ may interfere with the development of protective immune responses to tuberculosis during vaccination with mycobacterial proteins (21).

ACKNOWLEDGMENTS

This work was supported by grants POCTI/32629/99 and PSIDA/MGI/49647/2003 from the Portuguese Science and Technology Foundation (FCT, Portugal), SDH.IC.I.01.15 from the Calouste Gulbenkian Foundation (Portugal), and AI-41922 from the National Institutes of Health (NIH). M. Flórido and M. Borges received fellowships from the FCT.

We are indebted to J. Mudgett, J. Adams, and S. Holland for their gift of animal strains.

REFERENCES

1. **Busch, D. H., I. M. Pilip, S. Vijh, and E. G. Pamer.** 1998. Coordinate regulation of complex T cell populations responding to bacterial infection. Immunity **8:**353–362.
2. **Chen, W., W. Jin, H. Tian, P. Sicurello, M. Frank, J. M. Orenstein, and S. M. Wahl.** 2001. Requirement for transforming growth factor β1 in controlling T cell apoptosis. J. Exp. Med. **194:**439–453.
3. **Cooper, A. M., L. B. Adams, D. K. Dalton, R. Appelberg, and S. Ehlers.** 2002. IFN-γ and NO in mycobacterial disease: new jobs for old hands. Trends Microbiol. **10:**221–226.
4. **Dai, C., and S. Krantz.** 1999. Interferon γ induces upregulation and activation of caspases 1, 3, and 8 to produce apoptosis in human erythroid progenitor cells. Blood **93:**3309–3316.
5. **Dalton, D. K., L. Haynes, C.-Q. Chu, S. L. Swain, and S. Wittmer.** 2000. Interferon-γ eliminates responding CD4 T cells during mycobacterial infection by inducing apoptosis of activated CD4 T cells. J. Exp. Med. **192:**117–122.
6. **Ehlers, S., J. Benini, S. Kutsch, R. Endres, E. T. Rietschel, and K. Pfeffer.** 1999. Fatal granuloma necrosis without exacerbated mycobacterial growth in tumor necrosis factor receptor p55 gene-deficient mice intravenously infected with *Mycobacterium avium*. Infect. Immun. **67:**3571–3579.
7. **Ehlers, S., S. Kutsch, J. Benini, A. Cooper, C. Hahn, J. Gerdes, I. Orme, C. Martin, and E. T. Rietschel.** 1999. NOS2-derived nitric oxide regulates the size, quantity and quality of granuloma formation in *Mycobacterium avium*-infected mice without affecting bacterial loads. Immunology **98:**313–323.
8. **Flórido, M., M. Correia-Neves, A. M. Cooper, and R. Appelberg.** 2003. The cytolytic activity of natural killer cells is not involved in the restriction of *Mycobacterium avium* growth. Int. Immunol. **15:**895–901.
9. **Flórido, M., A. S. Gonçalves, R. A. Silva, S. Ehlers, A. M. Cooper, and R. Appelberg.** 1999. Resistance of virulent *Mycobacterium avium* to interferon-γ-mediated antimicrobial activity suggests additional signals for induction of mycobacteriostasis. Infect. Immun. **67:**3610–3618.
10. **Flórido, M., A. M. Cooper, and R. Appelberg.** 2002. Immunological basis of the development of necrotic lesions following *Mycobacterium avium* infection. Immunology **106:**590–601.
11. **Fulda, S., and K.-M. Debatin.** 2002. IFNγ sensitizes for apoptosis by upregulating caspase-8 expression through the Stat1 pathway. Oncogene **21:**2295–2308.
12. **Geng, Y., R. B. Shane, K. Berencsi, E. Gonczol, M. H. Zaki, D. J. Margolis, G. Trinchieri, and A. H. Rook.** 2000. *Chlamydia pneumoniae* inhibits apoptosis in human peripheral blood mononuclear cells through induction of IL-10. J. Immunol. **164:**5522–5529.
13. **Gilbertson, B., and C. Cheers.** 2002. Generalized immunological decline during long-term experimental infection with *Mycobacterium avium*. Infect. Immun. **70:**7145–7148.
14. **Gilbertson, B., J. Zhong, and C. Cheers.** 1999. Anergy, IFN-γ production, and apoptosis in terminal infection of mice with *Mycobacterium avium*. J. Immunol. **163:**2073–2080.
15. **Gomes, M. S., M. Flórido, T. F. Pais, and R. Appelberg.** 1999. Improved clearance of *Mycobacterium avium* upon disruption of the iNOS gene. J. Immunol. **162:**6734–6739.
16. **Gross, A., J. M. McDonnell, and S. J. Korsmeyer.** 1999. BCL-2 family members and the mitochondria in apoptosis. Genes Dev. **13:**1899–1911.

17. **Haynes, L., P. J. Linton, S. M. Eaton, S. L. Tonkonogy, and S. L. Swain.** 1999. Interleukin 2, but not other common gamma chain-binding cytokines, can reverse the defect in generation of CD4 effector T cells from naive T cells of aged mice. J. Exp Med. **190:**1013–1024.
18. **Hildeman, D., A., Y. Zhu, T. C. Mitchell, J. Kappler, and P. Marrack.** 2002. Molecular mechanisms of activated T cell death in vivo. Curr. Opin. Immunol. **14:**354–359.
19. **Hildeman, D. A., T. Mitchell, T. K. Teague, P. Henson, B. J. Day, J. Kappler, and P. C. Marrack.** 1999. Reactive oxygen species regulate activation-induced T cell apoptosis. Immunity **10:**735–744.
20. **Hirsch, C. S., Z. Toossi, J. L. Johnson, H. Luzze, L. Ntambi, P. Peters, M. McHugh, A. Okewera, M. Joloba, P. Mugyenyi, R. D. Mugerwa, P. Terebuh, and J. J. Ellner.** 2001. Augmentation of apoptosis and interferon-g production at sites of active *Mycobacterium tuberculosis* infection in human tuberculosis. J. Infect. Dis. **183:**779–788.
21. **Leal, I. S., B. Smedegård, P. Andersen, and R. Appelberg.** 2001. Failure to induce enhanced protection against tuberculosis by increasing T cell-dependent interferon-gamma generation. Immunology **104:**157–161.
22. **Liu, Y., and C. A. Janeway.** 1990. Interferon γ plays a critical role in induced cell death of effector T cell: a possible third mechanism of self-tolerance. J. Exp. Med. **172:**1735–1739.
23. **Locksley, R. M., N. Killeen, and M. J. Lenardo.** 2001. The TNF and TNF receptor superfamilies: integrating mammalian biology. Cell **104:**487–501.
24. **Mannering, S. I., and C. Cheers.** 2002. Interleukin-2 and loss of immunity in experimental *Mycobacterium avium* infection. Infect. Immun. **70:**27–35.
25. **Ogilvy, S., D. Metcalf, C. G. Print, M. L. Bath, A. W. Harris, and J. M. Adams.** 1999. Constitutive Bcl-2 expression throughout the hematopoietic compartment affects multiple lineages and enhances progenitor cell survival. Proc. Natl. Acad. Sci. USA **96:**14943–14948.
26. **Pais, T. F., J. F. Cunha, and R. Appelberg.** 2000. Antigen specificity of T-cell response to *Mycobacterium avium* infection in mice. Infect. Immun. **68:** 4805–4810.
27. **Pearl, J. E., B. Saunders, S. Ehlers, I. M. Orme, and A. M. Cooper.** 2001. Inflammation and lymphocyte activation during mycobacterial infection in the interferon-γ-deficient mouse. Cell. Immunol. **211:**43–50.
28. **Refaeli, Y., L. van Parijs, S. I. Alexander, and A. K. Abbas.** 2002. Interferon γ is required for activation-induced death of T lymphocytes. J. Exp. Med. **196:**999–1005.
29. **Roberts, A., A. Cooper, J. T. Belisle, and I. M. Orme.** 2002. Murine models of tuberculosis, p. 433–462. *In* S. H. E. Kaufmann and D. Kabelitz (ed.), Methods in microbiology: immunology of infection, ed. 2, vol. 32. Academic Press, London, England.
30. **Rocha, B., and H. von Boehmer.** 1991. Peripheral selection of the T cell repertoire. Science **251:**1225–1228.
31. **Silva, R. A., M. Flórido, and R. Appelberg.** 2001. Interleukin 12 primes $CD4^+$ T cells for interferon-γ production and protective immunity during *Mycobacterium avium* infection. Immunology **103:**368–374.
32. **Silva, R. A., T. F. Pais, and R. Appelberg.** 1998. Evaluation of interleukin 12 in immunotherapy and vaccine design in experimental *Mycobacterium avium* infections. J. Immunol. **161:**5578–5585.
33. **Silva, R. A., T. F. Pais, and R. Appelberg.** 2001. Blocking the receptor for interleukin 10 improves anti-mycobacterial chemotherapy and vaccination. J. Immunol. **167:**1535–1541.
34. **Teague, T. K., P. Marrack, J. W. Kappler, and A. T. Vella.** 1997. IL-6 rescues resting mouse T cells from apoptosis. J. Immunol. **158:**5791–5796.
35. **Varela, N., C. Munoz-Pinedo, C. Ruiz-Ruiz, G. Robledo, M. Pedroso, and A. Lopez-Rivas.** 2001. Interferon-γ sensitizes human myeloid leukemia cells to death receptor-mediated apoptosis by a pleiotropic mechanism. J. Biol. Chem. **276:**17779–17787.
36. **Wright, D. E., S. H. Cheshier, A. J. Wagers, T. D. Randall, J. L. Christensen, and I. L. Weissman.** 2001. Cyclophosphamide/granulocyte colony-stimulating factor causes selective mobilization of bone marrow hematopoietic stem cells into the blood after M phase of the cell cycle. Blood **97:**2278–2285.
37. **Zheng, L., G. Fisher, R. E. Miller, J. Peschon, D. H. Lynch, and M. J. Lenardo.** 1995. Induction of apoptosis in mature T cells by tumour necrosis factor. Nature **377:**348.
38. **Zhong, J., B. Gilbertson, and C. Cheers.** 2003. Apoptosis of CD4+ and CD8+ T cells during experimental infection with *Mycobacterium avium* is controlled by Fas/FasL and Bcl-2-sensitive pathways, respectively. Immunol. Cell Biol. **81:**480–486.

Editor: V. J. DiRita